Determination of the Critical-stress-intensity Factor K_{Ic} from Internally Pressurized Thick-walled Vessels

The critical-stress-intensity factor of thick-walled rock specimens is determined from the pressure at failure

by R. J. Clifton, E. R. Simonson, A. H. Jones and S. J. Green

ABSTRACT—Stable crack growth is obtained by subjecting prenotched thick-walled cylinders to internal pressure, with the bore jacketed to keep the crack faces traction free. The critical-stress-intensity factor K_{Ic} is determined from the pressure at failure. Results are presented for PMMA and a variety of rocks.

List of Symbols

a = inner cylinder radius (cm)
b = outer cylinder radius (cm)
E = Young's modulus (GPa)
G = energy-release rate (J/m^2)
l = nondimensional crack length
K_I = stress-intensity factor (MN/m$^{3/2}$)
K_I^* = nondimensional stress-intensity factor
K_{Ic} = critical-stress-intensity factor (MN/m$^{3/2}$)
L = crack length (cm)
p = internal pressure (MPa)
S = fracture-surface energy (J/m^2)
W = ratio of outer to inner radii
ν = Poisson's ratio
R = polar-coordinate radius
ζ = polar-coordinate angle
$\sigma_{\zeta\zeta}(R, \zeta)$ = normal-stress component in the ζ direction
$\sigma_{RR}(R, \zeta)$ = normal-stress component in the R direction

Introduction

The tensile strength of a rock is generally reported as the maximum tensile stress in a test specimen at the load which causes rupture. Test configurations commonly used include disks compressed diametrically by parallel platens, beams loaded in three- or four-point bending, and thick-walled cylindrical tubes subjected to internal pressure. From the point of view of fracture mechanics, the load at failure in these tests depends on the size, orientation and spacing of preexisting cracks and the rock's resistance to the extension of these cracks. Because the geometry of preexisting cracks is unknown and highly complex, such tests do not provide information which can be used to determine the rock's resistance to the extension of cracks. On the other hand, it is this resistance to crack extension that must be known if improved understanding of fracture development during hydraulic fracturing, underground testing and blasting is to be obtained.

A test configuration which shows promise for determining a rock's resistance to crack extension is that of a prenotched thick-walled cylinder subjected to internal pressure on the walls of the borehole but not on the faces of the notch. The advantages of this method are that: (1) the stress intensity at fracture need not be determined by the size of the crack at initial-crack extension, (2) the value of the stress-intensity factor at fracture should be obtained reliably from an accurate measurement of pressure at fracture and an approximate measurement of the crack length at fracture, and (3) core samples taken from field drill holes are readily made into test specimens by using the core directly and drilling only a small hole in the center. Analytical results regarding crack growth in this configuration were reported in Ref. 1. Herein, these results are reviewed and results of experiments using this configuration are reported. The analysis of Ref. 1 is also extended to include the practically important case of two diametrically opposed cracks.

The general approach in this work is to apply the

R. J. Clifton is associated with Brown University, Division of Engineering, Providence, RI 02912. E. R. Simonson, A. H. Jones and S. J. Green are associated with Terra Tek, Inc., Salt Lake City, UT 84108.

Paper was presented at 1975 SESA Spring Meeting held in Chicago, IL on May 11-16.

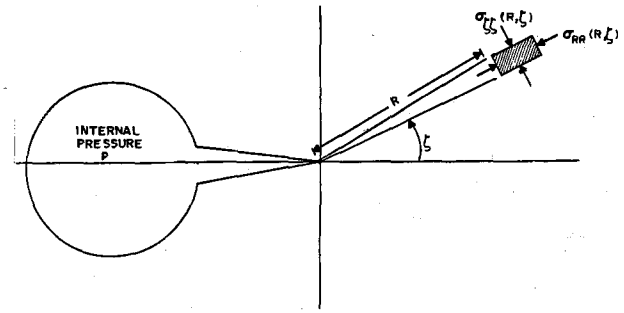

Fig. 1—Geometry of crack emanating from interior surface of a thick-walled cylinder

principles of linear-elastic fracture mechanics to the study of the tensile fracture of rocks. That is, linear-elastic material behavior is assumed everywhere except in a small region near the crack tip. The crack-tip region where inelastic deformations occur is assumed to be small relative to the crack length and other characteristic lengths associated with the applied loading. Then, the intensity of the loading experienced by the near-crack-tip region is determined by the strength of the singularity of the linear-elasticity solution at the crack tip (see, e.g., Rice[2]).

The singularity is one in which stresses near a sharp-crack tip are proportional to $R^{-1/2}$ where R is the distance from the crack tip. Thus, in linear-elastic fracture mechanics, the parameters to be evaluated, in order to determine whether or not a given crack will begin to extend under a given applied loading, are the so-called stress-intensity factors which are the coefficients of the singular terms (i.e., $R^{-1/2}$ terms) in the mathematical expansion of the stress state about the crack tip. For the case of radial-crack growth in a thick-walled cylinder under internal pressure, the stress field is symmetrical with respect to the crack plane, so that a purely opening mode or "Mode 1" type of crack extension would occur. The stress-intensity factor associated with this mode is denoted by K_I and is defined by:

$$K_I \equiv \lim_{R \to 0} (2\pi R)^{1/2} \sigma_{\zeta\zeta}(R, 0) , \qquad (1)$$

where $\sigma_{\zeta\zeta}(R, 0)$ is the normal stress perpendicular to the crack plane at a distance R from the crack tip, as shown in Fig. 1. The objective of the experiments is to determine the critical value of K_I at which crack extension occurs under the conditions of plane strain; this value is denoted by K_{Ic}.

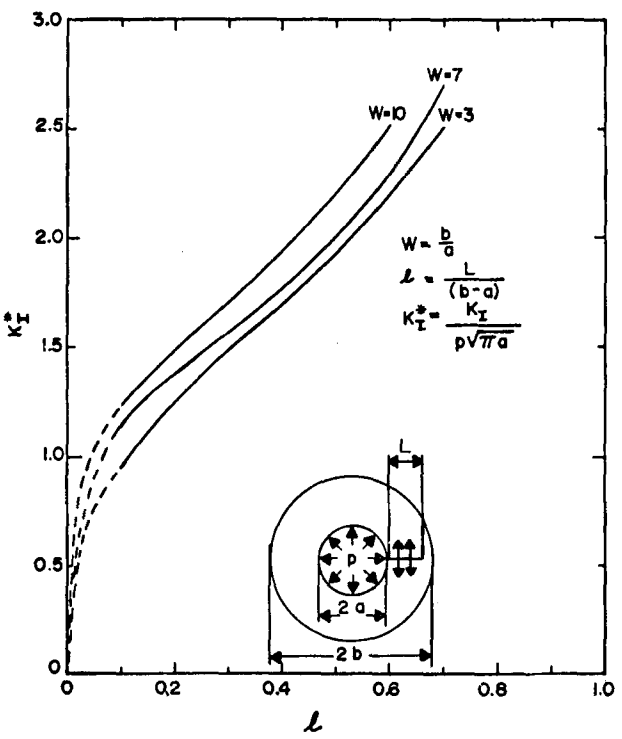

Fig. 2—Stress-intensity factor for unjacketed cylinder with a single radial crack

Stress-intensity Factors

Two types of internally pressurized cylinders must be distinguished in considering the stress-intensity factors associated with radial crack growth. One configuration, the so-called "unjacketed" case, involves no membrane between the pressurized fluid and the inner wall of the rock cylinder. In this case, the fluid pressure is regarded as acting on the newly developed crack surface as well as on the inner wall of the cylinder. In the other configuration, the "jacketed" case, a soft impermeable liner is placed inside the bore of the cylinder to prevent the fluid from entering cracks emanating from the inner wall of the cylinder. The analyses for the jacketed and unjacketed cases are considered separately.

Unjacketed Case

The stress-intensity factor for a thick-walled tube with a radial crack or cracks subjected to internal pressure, p, which also acts on the crack surfaces, is the same as for the case of uniform external tension acting on a tube of the same geometry with stress-free internal boundaries. The equivalence of the two loading cases follows immediately by noting that the former is obtained from the latter by superposition of a uniform hydrostatic pressure which negates the external tension (the stress-intensity factor is, of course, unchanged by the superposition of a uniform stress field). The latter problem has been solved by Bowie and Freese[3] by means of an approximate conformal mapping technique which preserves the sharpness of the crack tips and which is generally regarded as providing values for stress-intensity factors which differ from exact values by less than 0.1 percent.

In their published work,[3] Bowie and Freese consider only moderately thick cylinder walls for which the ratio $W = b/a$ of inner and outer radii is less than 2; however, they kindly agreed to provide numerical solutions for larger values of W.[4] The results are shown in Fig. 2 for the case of a single radial crack and, in Fig. 3, for two diametrically opposed radial cracks. Two features of the dependence of the dimensionless stress-intensity factor K_I^* on the dimensionless crack length $l = L/(b - a)$ (L is the crack length) shown in Fig. 2 and 3 have particular

significance in the interpretation of fracture tests on thick-walled cylinders. First, K_I^* is a monotonically increasing function of l. This means, for example, that once crack extension is initiated for a given crack size, the stress-intensity factor will increase further as the crack extends at constant pressure. A larger value for the stress-intensity factor will tend to cause further crack extension so that crack extension is unstable. That is, complete separation of the vessel can occur once the pressure is increased to the point where the stress-intensity factor is large enough for fracture initiation to occur. Crack growth could perhaps be stabilized or arrested if the expansion of the inner bore due to the crack opening caused a sufficient reduction in the internal pressure; also, the critical value of the stress-intensity factor which is necessary for crack extension may increase with distance of crack propagation and, thereby, contribute to stabilization of the crack. However, it appears likely that unjacketed tests involve unstable crack growth at the pressure necessary to initiate fracture.

The second feature to be noted in Figs. 2 and 3 is that the steepness of the curves indicates a very strong dependence of the stress-intensity factor on the length of the critical crack. Thus, a small change in length of the longest crack can result in a large change in the pressure needed to cause fracture. Unless initial cracks whose lengths are known accurately are put into the cylinders, it appears that there would be so much scatter in the burst pressure that the tests would not provide reliable information on the critical value of the stress-intensity factor.

The dashed segments of the curves in Figs. 2 and 3 are extrapolations of the data of Bowie and Freese.[4] The behavior for extremely small l should be predictable by superposition of the stress-intensity factor for the uniform tension of an edge-notched plate (Koiter[5]) and the equivalent problem of uniform pressure on the faces of a crack in an edge-notched plate Bueckner.[6] The uniform tension is taken to be the hoop stress σ_θ at the inner radius of the tube without cracks. That is (see, for example, Timoshenko and Goodier[7]):

$$\sigma_\theta = \frac{W^2+1}{W^2-1}p \tag{2}$$

from which Koiter's solution gives, as the stress-intensity factor due to the tension σ_θ, the value:

$$K_I = 1.13\left(\frac{W^2+1}{W^2-1}\right)p(\pi L)^{1/2} \tag{3}$$

where L is the crack length. The stress-intensity factor associated with the pressure, p, acting on the crack faces is, according to Bueckner's solution, given by:

$$K_I = 1.13\,p\sqrt{\pi L} \tag{4}$$

Superposition of eqs (3) and (4) and the introduction of dimensionless variables defined in Figs. 2 and 3 gives the following asymptotic expression for the dimensionless stress-intensity factor K_I^* at small values of l:

$$K_I^* \simeq \frac{1.13(W^2+1)}{(W^2-1)}(W-1)^{1/2}l^{1/2} \tag{5}$$

Equation (5) was used as a guide in the extrapola-

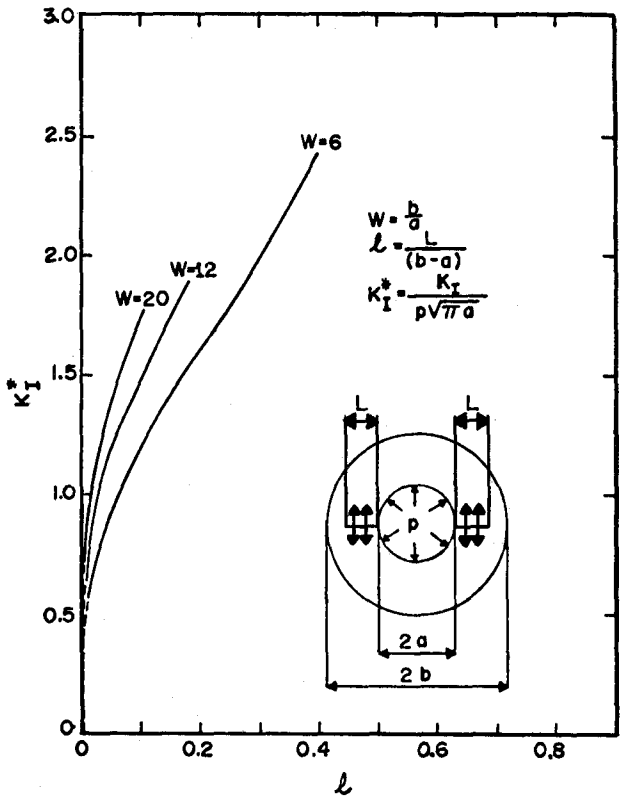

Fig. 3—Stress-intensity factor for unjacketed cylinder with two radial cracks

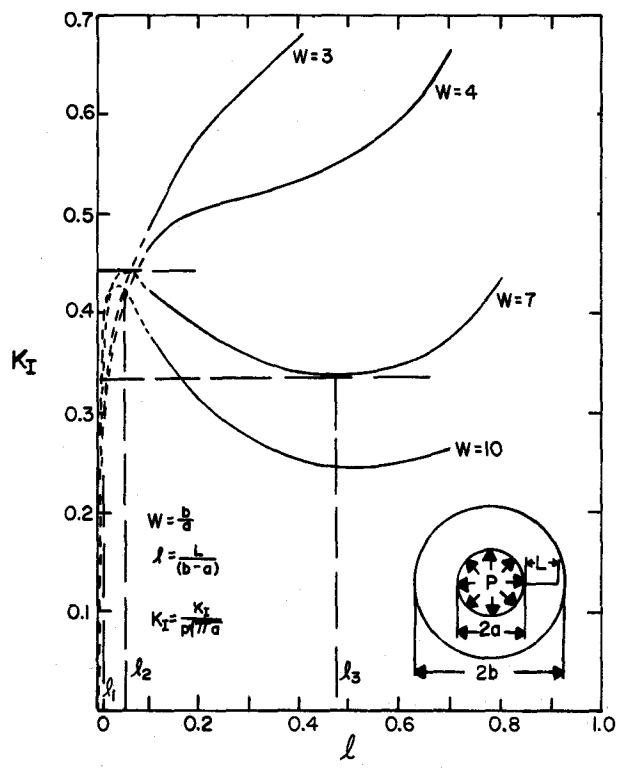

Fig. 4—Stress-intensity factor for jacketed cylinder with one radial crack

tion of the curves in Figs. 2 and 3 from the last data points to the origin.

Jacketed Case

When a soft liner is placed inside the bore of the cylinder, the appropriate boundary conditions are those of uniform pressure on the inner wall of the cylinder and zero traction on the faces of the radial crack or cracks. Bowie and Freese[4] have also been very helpful in providing numerical solutions under these conditions for the case of a single radial crack, Fig. 4, and the case of two diametrically opposed radial cracks, Fig. 5. The outstanding feature of the curves shown in these figures is that, for large values of the ratio W (say, W greater than 5 for the single-crack case and W greater than 10 for the double-crack case), the stress-intensity factor is not a monotonically increasing function of crack length. The negative slope segments of the curves suggest stable crack growth in that, after the extension of the crack, an increase in pressure is required to bring the stress-intensity factor back up to its original value. For the case of an infinite medium (i.e., $W = \infty$), Ouchterlony[8] evaluated the stress-intensity factor numerically as a function of crack length and observed that stable crack growth is predicted.

The various possibilities for stable and unstable crack growth can be summarized by referring to the case $W = 7$ in Fig. 4. If the initial crack length l_i is less than l_1, then unstable crack growth at constant pressure is likely. If $l_1 < l_i < l_2$, then initial crack growth should be unstable, but the crack would tend to be arrested before l reaches l_3. If $l_2 < l_i < l_3$, then stable growth with increasing pressure is expected for $l_i \leq l_3$. For $l_i > l_3$, unstable crack growth and final separation should occur without increase in pressure.

The preceding description of crack propagation should be interpreted as heuristic rather than as a statement of unquestionable necessary consequences of the dependence of K_I^* and l shown in Figs. 4 and 5. Possibly, important effects such as the effects of acceleration of the crack in regions of increasing K_I^* and decelerating in regions of decreasing K_I^* have not been discussed. Also, the influence of crack extension on the stress-intensity factor necessary for further crack extension has not been taken into account. Nevertheless, the existence of stable crack growth prior to the unstable crack growth which leads to separation is to be expected for jacketed cylinders with sufficiently large values for the ratio W. Furthermore, the existence of a broad minimum in the plots of K_I^* vs. l suggests that the stress-intensity factor (and consequently the pressure) at fracture should be reproducible from one experiment to another. Thus, experiments on jacketed cylinders have two important advantages over experiments on unjacketed cylinders: (1) the stress intensity at fracture need not be determined by the size of the crack at initial crack extension, and (2) the value of the stress-intensity factor at fracture should be obtained reliably from an accurate measurement of pressure at fracture and an approximate measurement of the crack length at fracture.

The dashed segments of the curves in Figs. 4 and 5 are obtained by extrapolation of the data of Bowie and Freese[4] and by requiring the asymptotic behavior at small l to be that of eq (3) or, in dimensionless

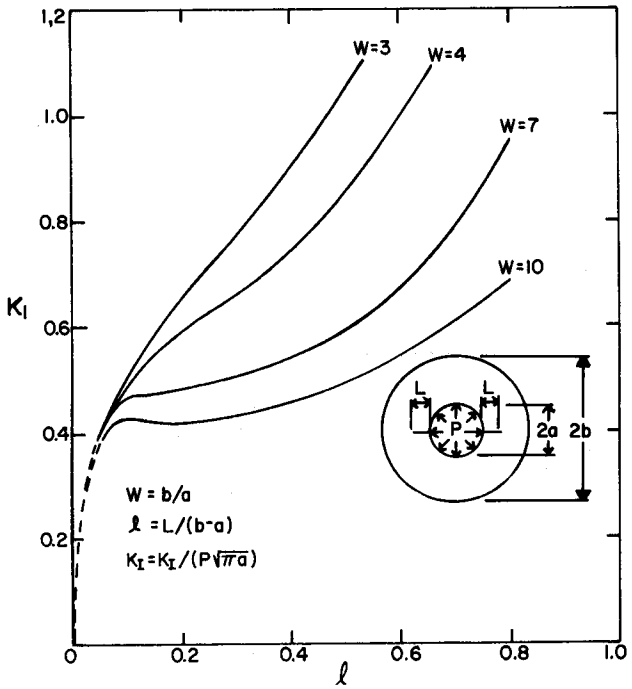

Fig. 5—Stress-intensity factor for jacketed cylinder with two radial cracks

form, the first term of eq (5). The general features of the extrapolated curves, including the fact that they cross, are believed to be reliable; however, in Fig. 4, the peak values of K_I^* for $W = 7$ and $W = 10$ are highly uncertain. Further calculations for $l < 0.1$ would be of value although the main region of interest is the region where K_I^* is a relative minimum. The latter region is well characterized by Fig. 4.

Experimental Methods and Results

Sample Preparation

Test specimens used in these studies were thick-walled cylinders of geologic material with an outer diameter of 10.16 cm and an inner diameter of 0.91 cm. Tests were also conducted on PMMA cylinders with an outer diameter of 10.16 cm and an inner diameter of 12.7 mm. All specimens were approximately 6.35 cm long with both ends ground flat and parallel to within 0.002 mm/mm. These dimensions give a wall ratio W (ratio of outer diameter to inner diameter, b/a) of 11.1 which, as shown in Fig. 5, should produce stable crack propagation provided the initial crack length lies in the interval 2.54 mm $< l/(b - a) <$ 5.08 mm. To this end, the thick-walled cylinders were precracked or, more precisely, prenotched to a depth corresponding to $l/(b - a) = 2.54$ mm or $L = 4.57$ mm. Precracking was accomplished with a diamond-impregnated copper wire, 0.203 mm in diameter. Two diametrically opposed radial cracks were inserted on the inside diameter along the full length of the cylinder. This technique produced a crack 0.23 mm wide. Fracture gages were applied on the flat surfaces at each end of the rock specimens. These gages were supplied by Micro-Measurements and are basically an array of very thin parallel wires similar

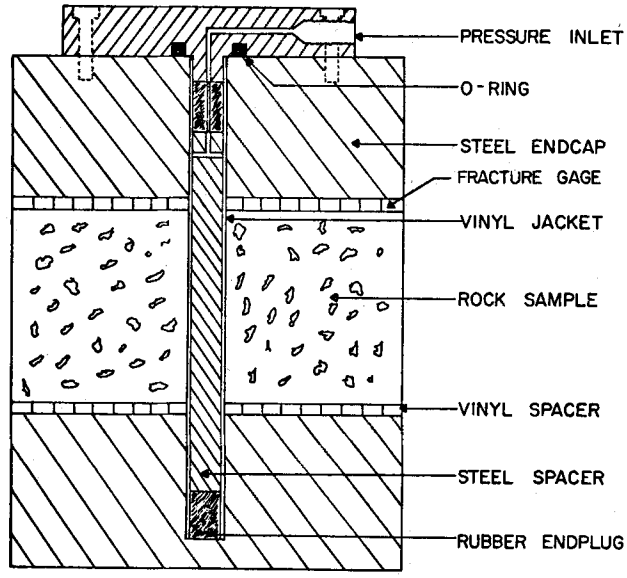

Fig. 6—Cross section of a typical burst-test specimen

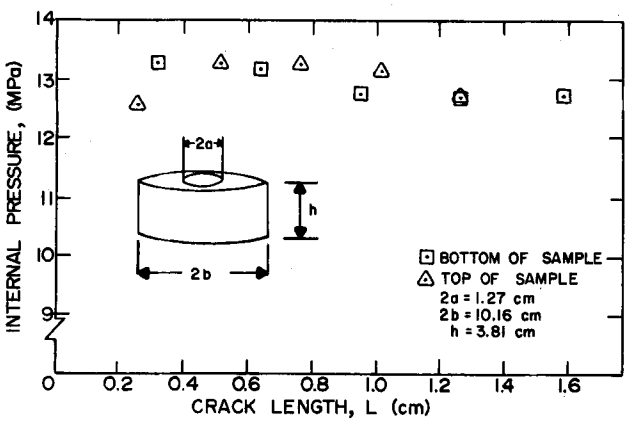

Fig. 7—Experimental measurement of internal pressure vs. crack length for a burst test on PMMA

to strain gages with all elements equally spaced with a separation of 0.13 mm. Figure 8 shows a schematic drawing of the fracture-gage placement on the ends of the test samples. Basically, as a fracture propagates into one of the arrays, successive wires will be cut, producing a loss in electrical continuity and providing an approximate measure of the crack-tip position. This technique proved useful to correlate crack-tip position as a function of internal pressure and to help answer the question of whether one or two cracks propagated as the specimen was pressurized.

Experimental Test Results

PMMA. As a check on the validity of this technique for determining K_{Ic} values for various materials, it was decided to first study polymethyl methacrylate (PMMA). Two important advantages are gained by studying this material. First, PMMA has been fully characterized as to its chemical and mechanical properties by many experimenters and, second, it is transparent and offers a visual inspection of the crack-propagation phenomenon. Several specimens were prepared as previously outlined, except that the cylinders were precracked to a depth of 1.02 mm due to technique limitations in these first tests. Internal pressure was slowly applied to the specimen until a crack was observed to propagate. As predicted by the analysis, the fracture was indeed stable and propagated to a distance of 2.54 mm before arresting. Two cracks were observed to propagate simultaneously. At this point, the pressure was manually decreased and the freshly fractured surface observed. The crack was almost planar and had propagated radially in the plane containing the precrack. The results were encouraging and the pressure was reapplied. When a critical pressure greater than the first pressure causing fracture was reached, the cracks extended once again and arrested at a crack length of approximately 5.08 mm. As before, the internal pressure was reduced and the fracture surfaces examined. This process was repeated until catastrophic failure occurred at a crack length of approximately 15.24 mm. These data are shown in Fig. 7. This particular sample had a wall ratio of about 8. For this ratio, and interpolating the data for $W = 8$ in Fig. 5, there is a broad minimum in the curve which suggests the pressure should only slightly increase over this stable region since $K_I^* \approx \text{const} = K_I/(p\sqrt{\pi a}) \rightarrow p \approx \text{const}$. The data show the pressure to increase initially by about 0.69 MPa as the crack extends from 1.02 mm to 5.1 mm and then decrease by 0.69 MPa until the fracture point is reached. If the value for K_{Ic}^* is taken to be the minimum of an interpolated curve for $W = 8$ in Fig. 5, then the value for K_{Ic} is easily determined to be

$$K_{Ic} = P_f\sqrt{\pi a}\, K_I^*$$

$$K_{Ic} = 12.7\ \text{MPa}\sqrt{\pi(.64)}\ (.45)$$

or

$$K_{Ic} = 0.810\ \text{MN/m}^{3/2}.$$

The value used for P_f was the pressure at which catastrophic failure occurred, i.e., $P_f = 12.7$ MPa. This value compares favorably with the value of 0.812 MN/m$^{3/2}$ reported by McClintock for cast PMMA at room-temperature conditions.[9] This value lends considerable credence to the burst-test approach for determining critical-stress-intensity factors by requiring only knowledge of the pressure at fracture.

ROCKS. Encouraged by the results of burst tests on PMMA, the technique was extended to geologic materials. The rock samples tested varied from coarse-grained sandstones with a porosity of 17 percent to fine-grained shales with a porosity of 0.2 percent. The wall ratio for these tests was 11.1 for an internal-bore diameter of 9.14 mm. In all cases, stable crack propagation was observed by means of fracture gages glued to the rock. These gages indicated that two cracks were extending on the rock and that crack extension was symmetric. This result is consistent with the calculation of K_I^* for the single- and double-crack case (see Figs 4 and 5) since a greater pressure is required to extend a single crack than a double crack.

The experimental results of burst tests on geologic materials at room temperature and pressure condi-

TABLE 1—SUMMARY OF BURST-TEST RESULTS ON GEOLOGIC MATERIALS

Rock Type*	Internal Radius, mm	Density, gm/cm³	Porosity, η (%)	Pressure At Failure, MPa	K_{Ic}, MN/m$^{3/2}$
SS	4.62	2.3	13.0	16.0	0.81
SS	4.57	2.32	7.9	11.3	0.57
SS	4.60	2.48	8.0	12.8	0.65
SS	4.60	2.49	6.8	28.9	1.46
SIL	4.62	2.42	9.5	20.6	1.04
SIL	4.60	2.65	4.4	27.1	1.37
SH	4.60	2.47	6.7	17.2	0.87
SH	4.62	2.59	0.2	18.8	0.95
SH	4.70	2.66	3.2	12.0	0.61
SH	4.70	—	—	25.3	1.29

* SS = Sandstone SIL = Siltstone SH = Shale

tions are listed in Table 1. The values reported for K_{Ic} were calculated from the results of a single test and do not represent an average over a series of tests. Additional tests on the same material will be required to establish the minimum number of tests required for repeatability.

Examination of the fracture surfaces after testing these rocks revealed some rather interesting results. The sandstones and siltstones showed smooth fracture surfaces as opposed to the shale samples which showed coarse, undulating surfaces. Fracture-surface roughness for the sandstones and siltstones was measured to be approximately ±1.27 mm while, for shale, the surface roughness was ±3.81 mm. This observation suggests that fractures in shales follow more tortuous paths than fracture in sandstones.

A soft impermeable jacket of Tygon tubing with a thickness of 1.52 mm prevents the pressurizing fluid from loading the crack faces and permeating the rock specimen. The jacket extends into steel end caps which are attached to each end of the sample. The seal for the pressurizing fluid is made in the steel end caps using the technique shown in Fig. 6. A small axial load causes the rubber end plug, placed between the end caps and the compression rod, to provide a fluid seal. The seal pressure is varied by changing the amount of interference between the steel end caps and the compression rod. A small steel tube in the upper rubber seal hydraulically connects the inner bore with the high-pressure line.

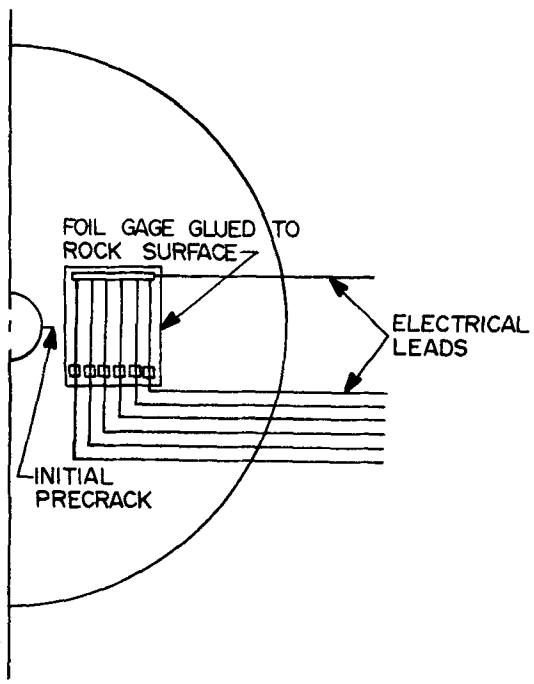

Fig. 8—Schematic drawing showing the placement of fracture gages on the end of a thick-walled-cylinder burst-test specimen

Conclusions

Analysis of crack propagation in thick-walled vessels with internal pressure has been examined from the point of view of linear-elastic fracture mechanics. For the particular case of a jacketed specimen in which the crack surfaces are traction free and pressure acts only on the borehole, calculations show a broad relative minimum in the plot of dimensionless stress-intensity factor vs. crack length for a cylinder with a diameter ratio greater than 7 for the case of one radial crack, and with a diameter ratio greater than 10 for the case of two radial cracks. The presence of this minimum suggests a region in which stable crack growth is possible at constant pressure. Experiments confirm the prediction of stable crack growth and support the usefulness of the jacketed, precracked thick-walled cylinder for studying tensile fracture of rocks. This configuration has the important feature that an accurate value of the critical-stress-intensity factor can be determined even when the crack length at fracture is known only roughly.

Acknowledgments

The authors would like to acknowledge Phil Randolph, Dean Power and Leo Rogers of El Paso Natural Gas Company for supplying the core samples and supporting the development of this technique; and Oscar Bowie and Collin Freese for their efforts in supplying K_I values for the single- and double-crack geometries.

References

1. *Johnson, J. N., Clifton, R. J., Simonson, E. R. and Green, S. J., "Analysis of Fracture of Hollow Cylindrical and Spherical Rock Specimens Subjected to Internal Pressure with Application to Underground Nuclear Containment," Terra Tek Rep. TR 73-50 (Sept. 1973).*

2. *Rice, J. R., "Mathematical Analysis in the Mechanics of Fracture," Ch. 3, Treatise on Fracture–Volume II, ed. by H. Liebowitz, Academic Press, New York 191 (1968).*

3. *Bowie, O. L. and Freese, C. E., "Elastic Analysis for a Radial Crack in a Circular Ring," Eng. Fract. Mech., 4 (2), 315-321 (June 1972).*

4. *Bowie, O. L. and Freese, C. E., Private communication.*

5. *Koiter, W. T., Disc. of "Rectangular Tensile Sheet with Symmetric Edge Cracks," by O. L. Bowie, J. Appl. Mech., 32, 237 (1965).*

6. *Bueckner, H. F., Boundary Problems in Differential Equations, ed. by R. E. Langer, Univ. of Wisconsin Press, Wisconsin 216 (1960).*

7. *Timoshenko, S. and Goodier, J. N., Theory of Elasticity, McGraw-Hill, New York (1951).*

8. *Ouchterlony, F., "Analysis av spanningstillstandet kring nagra olika geometrier med radiellt riktade sprickor, ett oa ndligt plant medium under inverkan av expansion skrafter," Internal Rep. to Swedish Detonic Res. Found. Vinterviken–11748 Stockholm (1972).*

9. *McClintock, F. A. and Argon, A. S., Mechanical Behavior of Materials, Addison-Wesley Publishing Co., Inc. (1966).*